The Role of Tryptophan Residues in the Function and Stability of the Mechanosensitive Channel MscS from *Escherichia coli*†

Akiko Rasmussen,‡ Tim Rasmussen,‡ Michelle D. Edwards, Daniela Schauer, Ulrike Schumann, Samantha Miller, and Ian R. Booth*

School of Medical Sciences, University of Aberdeen, Institute of Medical Sciences, Foresterhill, Aberdeen, AB25 2ZD, U.K.

Received May 30, 2007; Revised Manuscript Received July 19, 2007

ABSTRACT: Tryptophan (Trp) residues play important roles in many proteins. In particular they are enriched in protein surfaces involved in protein docking and are often found in membrane proteins close to the lipid head groups. However, they are usually absent from the membrane domains of mechanosensitive channels. Three Trp residues occur naturally in the *Escherichia coli* MscS (MscS-Ec) protein: W16 lies in the periplasm, immediately before the first transmembrane span (TM1), whereas W240 and W251 lie at the subunit interfaces that create the cytoplasmic vestibule portals. The role of these residues in MscS function and stability were investigated using site-directed mutagenesis. Functional channels with altered properties were created when any of the Trp residues were replaced by another amino acid, with the greatest retention of function associated with phenylalanine (Phe) substitutions. Analysis of the fluorescence properties of purified mutant MscS proteins containing single Trp residues revealed that W16 and W251 are relatively inaccessible, whereas W240 is accessible to quenching agents. The data point to a significant role for W16 in the gating of MscS, and an essential role for W240 in MscS oligomer stability.

Tryptophan is unique among the natural amino acids. It is not only the largest amino acid but has also complex chemical characteristics. The extended aromatic system accounts for its hydrophobicity, but the high electron density also results in energetically favorable interactions with positive charges, the cation−π interactions (*1*, *2*). On the other hand, the indole system has a permanent dipole moment because of the nitrogen atom, which is also responsible for the ability to form hydrogen bonds (*3*). This amphipathic character is especially important for membrane proteins where Trp is often found at the water−lipid interface, forming hydrogen bonds to the phospholipid head groups and dipping the remaining aromatic system into the lipid phase (*4*). Trp residues are enriched in binding hot spots at protein interfaces more than any other amino acid (*5*), indicating important roles in the stability of protein complexes. Last, the fluorescence properties of Trp enable the environment of the residue to be assessed from measurements of λ_{max} of the emission spectrum, the quantum yield (QY), and the accessibility to quenching agents. For this reason, Trp residues make good probes of protein conformation. To date, this technique has been applied to many ion channels, but has not been investigated for the mechanosensitive channel of small conductance, MscS.[1]

Bacterial mechanosensitive channels release solutes nonselectively in response to changes in the tension in the lipid bilayer. Such changes in tension are precipitated by the rapid inrush of water when cells transition from high to low osmolarity environments (*6*). The rapid release of solutes diminishes cell turgor and prevents cell lysis (*7*−*9*). In *Escherichia coli*, three different classes of mechanosensitive channels have been described (*8*, *10*) that open sequentially with increasing pressure. MscM (mechanosensitive channel of mini conductance) has the lowest conductivity and opens first. MscM has only been observed by electrophysiological experiments, and its molecular origin is unknown. MscS (small conductance) and MscK (potassium-dependent small conductance) (*11*) are members of the "MscS" family of proteins, and open at intermediate pressures, with MscK gating preceding that of MscS (*8*). At very high tensions, just below the point of membrane lysis, the mechanosensitive channel of large conductance, MscL, is triggered to open (*12*).

The MscS channel is the dominant activity in *E. coli* cells, in terms of both abundance and activity, and it alone can protect the cell against hypoosmotic shock (*8*). The MscS-Ec channel is a homoheptamer of 31 kDa subunits, each containing three Trp residues at positions 16, 240, and 251. Each subunit has three TM spans: TM1 (residues 27−57), TM2 (residues 68−91), and TM3. The pore-lining TM3 helix can be split into two portions, TM3A (95−112), a hydrophobic helix that forms the core of the pore, and TM3B (113−127), an amphipathic helix that connects the pore to

† This work was supported by Grant 040174 from The Wellcome Trust.

* To whom correspondence should be addressed. E-mail: i.r.booth@abdn.ac.uk. Phone: +44-1224-555852; Fax: +44-1224-555844.

‡ These authors equally contributed to this work.

[1] Abbreviations: BN, blue native; DDM, *n*-dodecyl-β-D-maltopyranoside; FRET, Förster (or fluorescence) resonance energy transfer; HEPES, 4-(2-hydroxyethyl)-1-piperazineethanesulfonic acid; IPTG, isopropyl-β-D-thiogalactoside; LB, Luria−Bertani; Leu, Leucine; MscS-Ec, mechanosensitive channel of small conductance from *Escherichia coli*; MOPS, 3-morpholinopropanesulfonic acid; Ni-NTA, nickel-nitrilotriacetic acid; Phe, phenylalanine; PMSF, phenylmethylsulfonylfluoride; PAGE, polyacrylamide gel electrophoresis; PBS, phosphate-buffered saline; PVDF, polyvinylidene fluoride; QY, quantum yield; SDS, sodium dodecyl sulfate; TM, transmembrane; Trp, tryptophan.

10.1021/bi701056k CCC: $37.00
Published on Web 08/24/2007

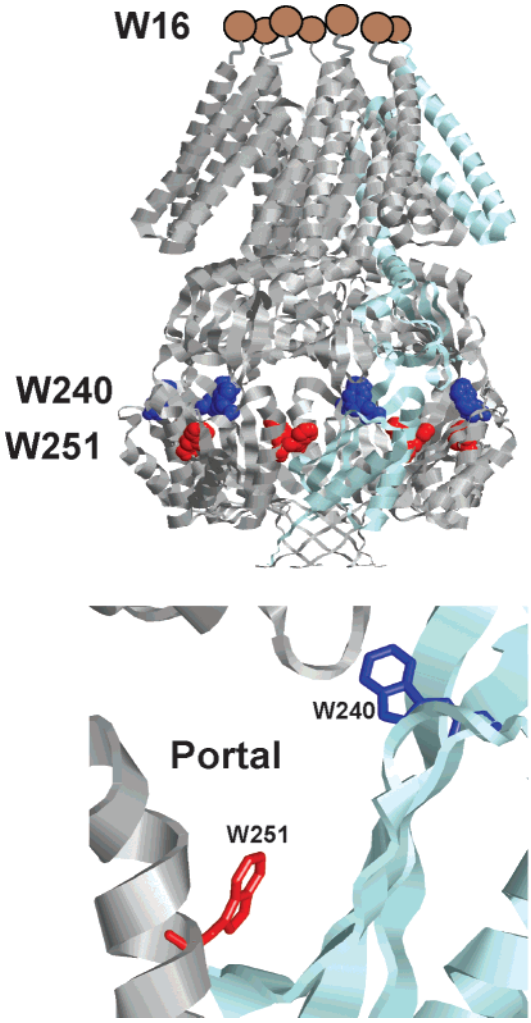

FIGURE 1: Location of tryptophan residues W240 (blue) and W251 (red) in MscS. Upper panel: The positions of W240 and W251, close to the side portals in the cytosolic domain, are shown in the context of the whole protein. The interface between two subunits (light blue and gray) is indicated to aid location of the portals. W16 is shown as a brown circle in the periplasmic region above the crystal structure to indicate that its precise location is not known. The distance between W240 and W251 from different subunits is 10 Å. Lower panel: An expansion of a single portal indicating the precise locations of W240 and W251. The images were made with RasTop on the basis of the crystal structure (*15*).

the carboxy-terminal vestibule domains. Trp residues are unusual in the membrane domains of mechanosensitive channels, and their introduction via mutagenesis can impair function (*13*). Little is known about the organization of the region surrounding W16 since this region was not resolved in the crystal structure, but it is about ten residues from the first TM region and thus may lie close to the membrane. The crystal structure (*14*, *15*) allows the positions of W240 and W251 in the channel complex to be defined with some precision. The cytoplasmic domain of MscS forms a large (~50 Å diameter) vestibule that is connected to the cytoplasm via seven lateral portals created by the domain interfaces. Both Trp residues are located close to the subunit interfaces in this large carboxy-terminal domain and therefore are close to the portals that penetrate the vestibule (Figure 1). Although the original structure did not place W240 at the portal, a registry error for the region of amino acids 226 to 244 has been discovered, revealing that W240 lies at the subunit interface (*15*).

Table 1: Primers Used for the Creation of Point Mutations

mutation	primers[a]
W16Y	5′−CggCgCgggA**TCCTAC**CTggTAgCTAACC-3′
W16F	5′−CggCgCgggA**TCCTTC**CTggTAgCTAACC-3′
W16L	5′−CggCgCgggA**TCCCTg**CTggTAgCTAACC-3′
W16Q	5′−CggCgCgggA**TCCCAg**CTggTAgCTAACC-3′
W16G	5′−CggCgCgggA**TCCggg**CTggTAgCTAACC-3′
W240L	5′−CgTggTCCg**AgTACTG**AgCAACAgCggC-3′
W251L	5′−gCAAAACgTgTAC**CTA**gATgTgCTgg-3′
W240F	5′−CgTggTCCg**AgTATTT**AgCAACAgCggCg-3′
W251F	5′−CgATCTgCAAAAC**gTC**TAC**TTT**gATgTgCTggAgCg-3′

[a] For each mutation only the forward primer is shown. As second primer the complementary sequence to the forward primer was used.

With the crystal structure as framework, we initiated fluorescence studies to understand structural changes during MscS-Ec gating. As a prerequisite to this goal, our initial study analyzed the native Trp residues by using mutant channel proteins where one or more Trp residues were exchanged against other hydrophobic amino acids. Using purified membrane proteins containing single Trp residues we have characterized the environment of the Trp residues and their contribution to MscS function and stability. Surprisingly, we observed that even a conservative change of W16Y increased the pressure required to gate MscS. Substitution of W240 with a Leu residue had a significant impact on MscS stability while exchanging this residue to Phe did not affect stability. We show that W251 and W16 are relatively inaccessible in the purified channel complex, but become accessible when the heptamer is dissociated into a mixture of monomer and dimer. Our data indicate important roles for W240 and W16, but less significance for W251. However, we demonstrate that Trp-free mutants, in which the three Trp residues are replaced by other aromatic amino acids, are functional and are stable in a solubilized state.

EXPERIMENTAL PROCEDURES

Materials. *n*-Dodecyl-*β*-D-maltopyranoside (DDM), sol-grade was obtained from Anatrace, Inc. All other chemicals were obtained from Sigma.

Bacterial Strains and Plasmids. *E. coli* strain MJF429 (Δ*mscS*, Δ*mscK::Kan*) has been used for the electrophysiological studies while MJF465 (Δ*mscL::Cm*, Δ*mscS*, Δ*mscK::Kan*) was used for all other experiments (*8*). Plasmid pTrcMscSH$_6$ was described previously (*16*).

Site-Directed Mutagenesis. The Stratagene QuikChange protocol was used to introduce point mutations into pTrcMscSH$_6$ or templates derived from this plasmid (*16*). The primers used to create the mutants in this study are summarized in Table 1. In addition to the amino acid change, a restriction site was introduced to facilitate the screening. The mutant plasmids were sequenced on both strands to verify that the only changes were those introduced by the mutagenic primers.

Downshock Experiments. The survival assay of osmotic downshock was essentially the same as described previously (*17*). Cells were grown at 37 °C in Luria−Bertani medium (LB) containing per liter: 10 g of tryptone, 5 g of NaCl, and 5 g of yeast extract; for LB-agar plates, 14 g of agar per liter was added to the medium. All survival experiments were performed using transformants of MJF465, and both induced (0.3 mM isopropyl-*β*-D-thiogalactoside [IPTG] added when

$OD_{650nm} \approx 0.2$) and noninduced cultures were studied. The culture was adapted to high osmolarity by growth to an OD_{650nm} of 0.4 in the presence of 0.5 M NaCl, and an osmotic downshock was then applied by a 1:20 dilution into LB medium (shock) or the medium containing 0.5 M NaCl (control). After 10 min incubation at 37 °C, 5 μL serial dilutions of these cultures were spread onto LB-agar plates in the presence (control) or absence (shock) of 0.5 M NaCl. The survival rates were then assessed by counting the number of colonies grown after incubation overnight at 37 °C. Data are reported as means ± standard deviation.

Electrophysiology. Patch clamp recordings were conducted on giant protoplasts as described previously (*18*, *19*) using the strain MJF429 (*8*) transformed with the MscS plasmids. Expression was induced with 1 mM IPTG for 15−30 min before protoplast generation. Excised, inside-out patches were analyzed at a membrane potential of −20 mV with pipet and bath solutions containing 200 mM KCl, 90 mM $MgCl_2$, 10 mM $CaCl_2$, and 5 mM HEPES buffer at pH 7. All data were acquired at a sampling rate of 50 kHz with 5 kHz filtration using an AxoPatch 200B amplifier and pClamp software (Axon). The pressure threshold for activation of the MscS channels was referenced against the activation threshold of MscL (P_L:P_S) to determine the pressure ratio for gating as previously described (*24*−*26*). Measurements have been conducted on patches derived from at least two protoplast preparations, and data were recorded from a minimum of four separate patches ($n = 4$ to 10 per channel). Pressure ratios are given as mean ± SEM; Student's *t*-test was used for determining significance.

Membrane Preparations and Western Blots. Western blots were performed on membrane preparations from IPTG-induced cells (0.3 mM, 30 min) as described (*16*). Membrane proteins (15 μg per track) were separated using preformed Novex NuPAGE 10% Bis-Tris SDS−PAGE gels with MOPS running buffer (Invitrogen) and transferred to nitrocellulose. Anti-His_6 antibody (mouse IgG2a isotype, Sigma) was used to probe the blot, and images were developed by ECL (Pierce) on photographic film (Kodak).

Expression and Purification. The different MscS constructs were transformed into the *E. coli* strain MJF465. Cells were grown in 500 mL of LB medium at 37 °C to an $OD_{650nm} \approx 0.8$. The cultures were cooled to 25 °C for 30 min and induced with 0.8 mM IPTG for 4 h. The cell pellet was resuspended in 12 mL of PBS buffer (phosphate-buffered saline buffer, pH 7.5: containing 8 g of NaCl, 0.2 g of KCl, 1.15 g of $Na_2HPO_4 \cdot 7H_2O$, and 0.2 g of KH_2PO_4 per liter), supplemented with 0.2 mM freshly prepared phenylmethylsulfonylfluoride (PMSF). After disruption of the cells with a French press at 18,000 psi, the suspension was centrifuged at 3000*g* for 20 min to remove cell debris. The supernatant was then centrifuged at 100000*g* for 1 h. The membrane pellet was resuspended in buffer A (1.5% DDM, 50 mM sodium phosphate pH 7.5, 300 mM NaCl, 10% glycerol, 50 mM imidazole, 0.2 mM PMSF) and incubated for 1 h at 4 °C. Aggregates were removed by centrifugation at 3000*g* for 10 min, and 0.5 mL of nickel-nitrilotriacetic acid (Ni-NTA) agarose was added to the supernatant. After incubation overnight at 4 °C, the suspension was transferred to a 5 mL plastic column and afterward washed with 40 mL of buffer B (0.05% DDM, 50 mM sodium phosphate pH 7.5, 300 mM NaCl, 10% glycerol, 50 mM imidazole, 0.2 mM PMSF). The elution followed with 10 mL of buffer C (as buffer B but with 300 mM imidazole) and 1 mL fractions were collected. The fractions were analyzed by SDS−PAGE and UV/vis absorption spectroscopy. This protocol produces protein of similar quality to that recently described (*20*).

Size Exclusion Chromatography. The two fractions with the highest protein content from the Ni-NTA column (see Expression and Purification) were applied to a 106 mL Hiprep Superdex 200 column (General Electrics Healthcare) equilibrated with buffer D (0.025% DDM, 50 mM sodium phosphate pH 7.5, 150 mM NaCl). MscS was eluted with buffer D at 1 mL/min. Protein concentration was monitored by absorption at 280 nm. The column was calibrated with the following standards: dextran blue (2 MDa, exclusion volume), thyroglobin (669 kDa), apoferritin (440 kDa), aldolase (161 kDa), ovalbumin (45 kDa), and carbonic anhydrase (29 kDa).

Blue Native (BN) PAGE. The DDM concentration of the samples for the BN PAGE was adjusted to 0.5%, and shortly before the sample application, 0.15% Coomassie G250 was added. Preformed native Novex 4−16% Bis-Tris gels (Invitrogen) were used and run at 150 V for 2 h. 50 mM BisTris/Tricine (pH 7.5) was used as running buffer. The cathode buffer contained additionally 0.02% Coomassie G250 in the first third of the run, which was then exchanged against a buffer containing only 0.002% Coomassie G250 for the remainder of the run. Proteins were then blotted on polyvinylidene fluoride (PVDF) membranes (Hypbond-P, Amersham Biosciences) and detected as described for the SDS−PAGE. The Native Mark unstained protein standard (Invitrogen) was used to determine molecular masses: IgM hexamer (1236 kDa), IgM pentamer (1048 kDa), apoferritin band 1 (720 kDa), apoferritin band 2 (480 kDa), β-phycoerythrin (242 kDa), lactate dehydrogenase (146 kDa), bovine serum albumin (66 kDa), and soybean trypsin inhibitor (20 kDa).

Fluorescence Spectroscopy. Fluorescence spectra were recorded with a FLS920 spectrometer (Edinburgh Instruments). The purified MscS samples solubilized in buffer D were diluted to an absorption of 0.050 at 295 nm to exclude an inner filter effect. The emission spectra were recorded with an excitation at 295 nm and an excitation slit width of 1 nm while the emission slit was set to 2 nm. The spectra were then normalized to the same MscS concentrations to allow a direct comparison. The concentrations were calculated from the absorption at 280 nm using extinction coefficients given by the protein calculator on the basis of the amino acid content (*21*). The fluorescence spectrum of the mutant W16F/W240F/W251F, which contains no Trp, was taken as background spectrum accounting for scattering. Quantum yields (QY) were calculated, assuming that the refractive index is unchanged between samples and standard, as follows:

$$QY = QY_{st} \cdot I/I_{st} \cdot A_{st}/A$$

where QY and QY_{st} are the quantum yields of the sample and the standard, respectively, I and I_{st} are the integrated intensities of the fluorescence for sample and standard, and A and A_{st} are the absorptions at 295 nm. A free Trp solution in H_2O was used as standard assuming a QY_{st} of 0.14 (*22*).

Quenching experiments were performed on a Shimadzu RF1501 fluorescence spectrometer. An excitation wavelength

Table 2: Properties of MscS-Ec Trp Mutants[a]

MscS mutant	Trp positions 16	240	251	P_L:P_S ratio[b]	λ_{max} (nm)	quantum yield
WT	+	+	+	1.64 ± 0.02	333	0.28 ± 0.03
W16Y	−	+	+	1.44 ± 0.02***	333	0.32 ± 0.03
W16F	−	+	+	1.28 ± 0.03***	333	0.33 ± 0.01
W16L	−	+	+	1.20 ± 0.02***	nd	nd
W16Y/W240F	−	−	+	1.32 ± 0.04***	327	0.09 ± 0.02
W16F/W240F	−	−	+	1.28 ± 0.02***	327	0.12 ± 0.01
W16F/W251F	−	+	−	1.24 ± 0.03***	334	0.36 ± 0.05
W240F	+	−	+	1.53 ± 0.04^{NS}	329	0.13 ± 0.01
W240L	+	−	+	1.49 ± 0.04**	327	0.11 ± 0.02
W251F	+	+	−	1.51 ± 0.04^{NS}	333	0.29 ± 0.02
W251L	+	+	−	1.57 ± 0.02^{NS}	333	0.25 ± 0.08
W240F/W251F	+	−	−	1.53 ± 0.03^{NS}	325	0.08 ± 0.01
W16F/W240F/W251F	−	−	−	1.24 ± 0.03***	na	na
W16Y/W240F/W251F	−	−	−	1.34 ± 0.03***	na	na

[a] P_L:P_S ratios were measured for each mutant channel in strain MJF429 (MscL$^+$) as described in Experimental Procedures. Quantum yield and λ_{max} were determined for the MscS protein(s) purified in DDM using the heptameric fraction (see Figure 4). Abbreviations: nd, not determined; na, not applicable. [b] The mean P_L:P_S ratio for each channel was compared with that of the wild type using the Student's unpaired *t*-test (NS, $P > 0.01$; **, $P < 0.01$; ***, $P < 0.001$).

of 295 nm was used with an excitation and emission slit width of 10 nm. The quenchers were dissolved in the same buffer as MscS (buffer D), and the concentrations of the stock solutions were 1 M for acrylamide and 5 M for KI and CsCl. In the case of KI, 0.1 mM of $S_2O_3^{2-}$ was added to prevent I_3^- ion formation.

RESULTS

MscS in *E. coli* contains three Trp residues at positions 16, 240, and 251. Of the three residues W16 and W240 are highly conserved; W16 is conserved in 60% of the top 100 proteins showing strong overall similarity to MscS-Ec by BLAST (*23*), with an aromatic amino acid being present in 87% of homologues. W240 is conserved in almost 100% of MscS proteins. In contrast, W251 is more frequently encountered as Phe (57%) and only 29% of the closest relatives of MscS-Ec have Trp at this position. To investigate the importance of Trp residues, and to gain insights into their environments in purified MscS, we created mutations at these positions, replacing Trp with Phe or Leu. In addition, we have previously described a series of mutations at W16 that convert this residue to Tyr, Phe, Leu, Gly, and Gln (*16*), and these were further characterized in this study.

Properties of Trp Mutant Channels. The properties of mutant channels can be analyzed by assessing their ability to assemble in the cytoplasmic membrane, by their electrophysiological characteristics, and by their physiological function in protecting cells against hypoosmotic shock (*16*, *19*, *24*). We have previously demonstrated normal expression and incorporation in the membrane of W16Y, W16F, W16Q, W16G, and W16L mutant proteins, with the lowest incorporation being exhibited by W16G (*16*). Similarly, protection against hypoosmotic shock was afforded by all five mutants when highly expressed (*16*). This analysis has been extended by electrophysiology, which has revealed significant changes in gating pressure associated with W16 mutations (Table 2).

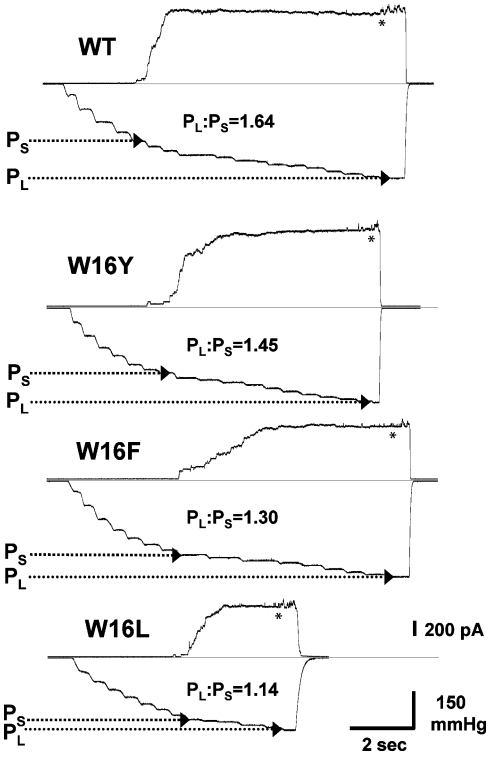

FIGURE 2: Substitution of the tryptophan at position 16 affects gating pressure threshold. Membrane patches of protoplasts derived from strain MJF429 expressing wild type or mutant MscS protein were analyzed by patch clamp at a membrane potential of −20 mV, as described in Experimental Procedures. A representative trace is shown for each, along with its specific P_L:P_S ratio. The upper panel of each trace is the current recorded, and the lower panel is the negative pressure applied to the patch. Arrows denote the pressure level taken as measurement for either MscS or MscL openings; note the decreasing gap between pairs of arrows as the P_L:P_S ratio decreases. * indicates where regular MscL openings begin. The figure shows example traces for wild type (WT) MscS, W16Y, W16F, and W16L channels.

The pressure required to activate the MscS mutant channels in membrane patches is expressed relative to that required to gate MscL, the P_L:P_S ratio (*24*−*26*), as previously shown (*19*). The pressure required for gating W16 mutant channels was increased significantly relative to wild type (e.g., W16L, P_L:P_S = 1.20 ± 0.02 compared with 1.64 ± 0.02 for wild type, $P < 0.001$, $n > 5$). We found that the pressure sensitivity was determined by the character of the amino acid substitution: the P_L:P_S ratio decreased in the series wild type > W16Y > W16F > W16L (Figure 2; Table 2). However, current traces of all mutant channels showed wild type profiles, with wild type-like conductance and stable openings and no loss of the desensitization characteristic typical of MscS-Ec channels (data not shown).

Mutations affecting W251 or W240 had distinctive phenotypes that reflected the retention or loss of the aromatic character of the amino acid placed at these positions. Expression of the mutant channels did not affect growth at either low or high osmolarity (data not shown). However, introduction of a Leu in position 240 resulted in lower abundance in membranes whereas W240F, W251F, and W251L were expressed normally and accumulated to similar levels to the wild type protein. The effect seen with W240L was augmented by a W251L mutation since the double mutant, W240L/W251L, was only present in membranes at very low levels (Figure 3A). The presence of the W240L

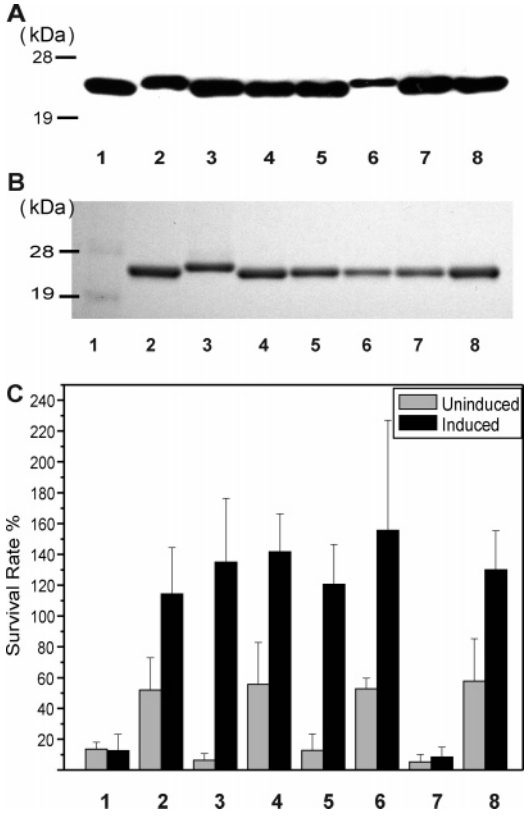

FIGURE 3: Properties of MscS tryptophan mutants. (A) Western blot of membrane proteins using anti-His_6 antibodies: 1, WT; 2, W240L; 3, W240F; 4, W251L; 5, W251F; 6, W240L/W251L; 7, W240F/W251F; 8, WT. (B) Coomassie blue-stained SDS−PAGE of purified MscS mutants, which were adjusted to equal concentrations: 1, markers; 2, WT; 3, W240L; 4, W240F; 5, W251F; 6, W251L; 7, W240F/W251F; 8, WT. (C) Ability of tryptophan mutants to survive a hypoosmotic shock. Gray bars indicate experiments with noninduced cells, and black bars, with induced cells (0.3 mM IPTG). Data shown are the mean values ± standard deviation of at least four independent experiments: 1, MJF465; 2, WT; 3, W240L; 4, W240F; 5, W251L; 6, W251F; 7, W240L/W251L; 8, W240F/W251F. Strain MJF465 was used as the control and lacks MscS, MscK, and MscL; data sets 2−8 are MJF465 transformed with $pTrcMscSH_6$ bearing the appropriate mutation(s). Further experimental details can be found in the Experimental Procedures.

mutation also caused a pronounced modification of the mobility of the MscS-Ec protein on SDS−PAGE gels (Figure 3A). This feature was retained after the protein had been purified (Figure 3B) (see below) suggesting a significant conformational change in the channel complex arising from the Leu substitution at residue 240. These features were reflected in the physiological activity of the channels. Channels with Phe introduced in place of Trp protected against hypoosmotic shock in a similar manner to the wild type protein (Figure 3C) and displayed essentially wild type properties in patch clamp analysis (Table 2). In contrast, protection by W240L was only observed when the protein was overexpressed. This lack of protection by basal levels of W240L MscS channels most probably reflects lowered protein abundance rather than loss of channel activity since the mutant channels were observed to gate in electrophysiological experiments (Figure 2). The double mutant W240L/W251L failed to protect even when induced (Figure 3C). These data are consistent with the observed expression patterns (Figure 3A). Trp-free mutant channels were constructed that either had Phe in all three positions or had Tyr at position 16 and Phe at 240 and 251. The triple mutant channel with closest properties to wild type MscS-Ec possessed Tyr at position 16 and Phe at positions 240 and 251 (Table 2).

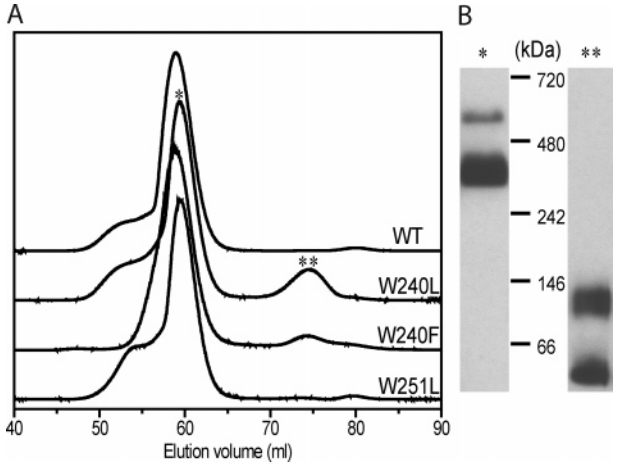

FIGURE 4: MscS W240L is less stable during purification than either native protein or other tryptophan mutants. (A) Size exclusion chromatography of MscS wild type (WT), W240L, W240F, and W251L. The graphs are normalized and offset for clarification. (B) Blue native PAGE of MscS W240L. The samples were taken from the size exclusion chromatography as indicated by the asterisks.

Expression, Purification, and Molecular Characterization of Mutant MscS. To reveal why the Trp mutations have an effect on the functionality of MscS, we assessed the oligomeric state of the purified proteins by size exclusion chromatography and used the natural fluorescence of Trp for spectroscopic investigations. With the single exception of the W240L/W251L double mutant, all of the MscS proteins could be purified at yields similar to wild type MscS. MscS was solubilized with DDM and purified on a Ni-NTA agarose column, using the carboxy-terminal His_6-tag. The oligomeric state of the solubilized MscS was then assessed by size exclusion chromatography (Figure 4A). It should be noted that identical results were obtained with DDM concentrations between 0.015% and 0.05%, as well as with Foscholine-14 (0.01%), but octylglucoside (1%) was observed to cause aggregation of MscS (data not shown).

MscS was detected in fractions of two peaks: the main peak eluted at 60 mL and the small peak at 75 mL (Figure 4A). Molecular weights of 350 kDa and 80 kDa were estimated, respectively, by utilizing a calibration with soluble proteins (see Experimental Procedures section). The mass of the main peak, 350 kDa, is much higher than the calculated mass for the heptameric MscS (217 kDa). The apparent mass of the heptamer is expected to be higher than the calculated value because of bound detergent and phospholipids. A sample of the peak was applied to blue native (BN) PAGE (Figure 4B), which was also calibrated with soluble proteins. The main peak in the BN gel showed a strong band at 370 kDa. For many different transporters a correction factor (1.8) has been calculated that accurately corrects the mass observed on BN gels for bound detergent and lipids relative to masses of soluble standards (*27*). Applying this factor to this MscS band, a mass of 206 kDa was estimated for the detergent-free complex which is close to the calculated mass of 217 kDa for the heptamer. Therefore, we attribute the main peak to the heptameric form of MscS. Another faint band at 611

kDa (corrected 340 kDa) was also seen in the samples derived from the main peak. The molecular origin of this band is not clear but might be caused by protein aggregation (*15*, *27*). The small peak, estimated mass of 80 kDa in the size exclusion chromatography, also shows two bands on the BN PAGE, with estimated masses of 56 kDa (corrected 31 kDa) and 104 kDa (corrected 58 kDa). We attribute this peak to dissociated MscS containing a mixture of the monomeric and dimeric forms. All preparations of MscS showed a high content of the heptameric form and only small amounts of dissociated MscS. However, for the mutant W240L we found a significantly increased amount of monomer, consistent with a slight loss of stability associated with this mutation, as indicated by lowered accumulation in the membrane (Figure 3A). The main peak containing the heptameric MscS was used for further experiments.

Fluorescence of the Natural Tryptophan Residues in MscS. The intrinsic fluorescence of Trp can be used to obtain information about the environment of these residues and can reveal interactions and conformational changes. Therefore, we studied purified MscS and its mutated forms by fluorescence spectroscopy. We compared the fluorescence of the WT with mutants that possess a single Trp residue. All spectra were normalized to the same MscS concentration to show the contribution of the single Trp residue to the wild type fluorescence spectrum. The mutant MscS W240F/W251F contains only W16, for which one cannot readily predict the molecular environment because the N-terminal region between residues 1 and 26 is not resolved in the crystal structure (*14*). The maximum of fluorescence for this Trp residue (λ_{max} = 325 nm) is blue-shifted (Figure 5A) in comparison to Trp residues located at the protein surface or to free Trp in solution (λ_{max} = 348 nm on our spectrometer). This indicates that W16 is located in a hydrophobic environment, not exposed to the water phase. The low quantum yield suggests that the fluorescence of W16 is quenched by the surrounding protein matrix (*28*) (Table 2).

W251 is located directly at the side portal and is in contact with the neighboring subunit. For W251 (MscS mutant W16F/W240F), λ_{max} is again blue-shifted but to a slightly lesser extent than W16 and the quantum yield is low (Figure 5; Table 2). The crystal structure shows that the indole group of W251 is on the lower edge of the portal where an α helix of one subunit packs against the β sheet of the adjacent subunit. The W251 residue of subunit A is surrounded by Asn (248:A and 226:G) and Gln (247:A) residues as well as having potential cation−π interactions via R224:G (*15*). This environment predicted from the crystal structure is consistent with the low quantum yield (*28*).

Analysis of W240 (MscS W16F/W251F) suggests that this residue is the dominant contributor to the wild type fluorescence. The emission maximum is red-shifted in comparison to W16 and W251 (λ_{max} = 334 nm; Figure 5), which indicates a more polar environment, and is almost identical to the wild type protein (Table 2). The quantum yield determined for W240 is very high in comparison to Trp residues in other proteins, indicating that the quenching by the protein matrix is low (*28*, *29*).

Summation of the individual spectra from the single Trp mutants gives a spectrum that is lower than the wild type spectrum (Figure 5A). This can be explained by a Förster (or fluorescence) resonance energy transfer (FRET) between

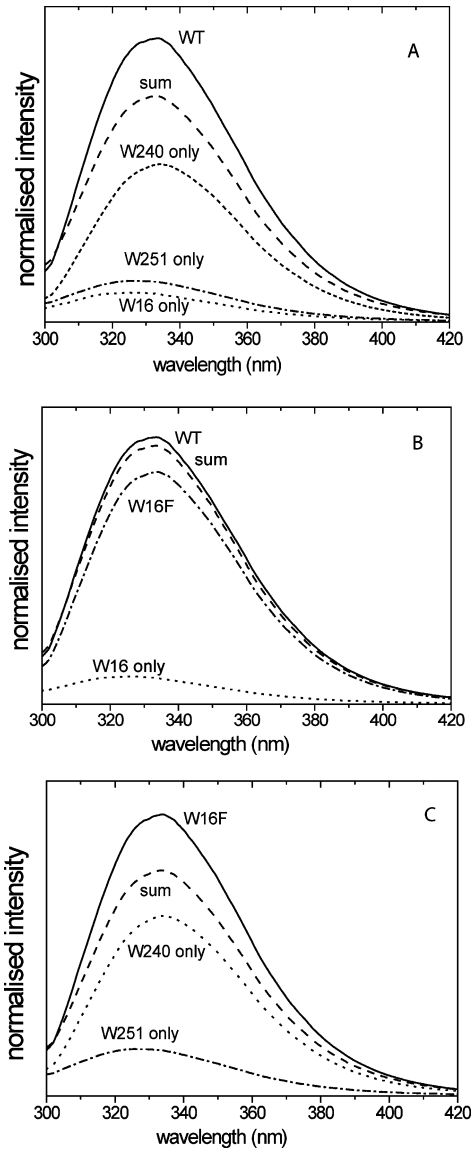

FIGURE 5: Fluorescence spectra of purified MscS. All spectra were recorded at the same absorbance of 295 nm but were afterward normalized to protein concentration. (A) The WT spectrum (solid) is compared with the sum (dash) of spectra from mutants containing only a single tryptophan: W16 (dot), W240 (short dash), and W251 (dot−dash). (B) The WT spectrum (solid) is shown together with the sum (dash) of W16F (dot−dash) and W240F/W251F (W16 only; dot). (C) The W16F spectrum (solid) is shown together with the sum (dash) of the single tryptophan proteins W240 (dot) and W251 (dot−dash).

W251 and W240 (*30*). These Trp residues are only 10 Å apart in the most recent crystal structure (*15*), allowing an efficient energy transfer. FRET will mainly take place from blue-shifted W251 to W240 because of the spectral overlap of the Trp absorption spectra, and the emission spectrum of W251 is bigger than for W240. The transferred energy will emerge as fluorescence because W240 is less quenched than W251, which has alternative relaxation pathways. In the mutants with single Trp residues, no energy transfer can take place, explaining why the sum spectrum is lower than the wild type spectrum. Other sum spectra confirm this explanation: a sum spectrum of W240 and W251 from proteins with single Trp residues at these positions is lower than the spectrum of the mutant containing both W240 and W251 (Figure 5C). However, a spectrum of the protein containing

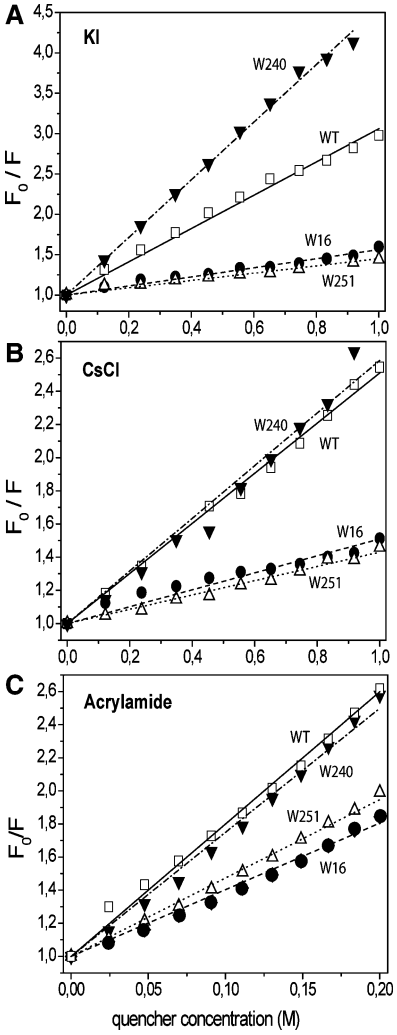

FIGURE 6: Stern−Volmer plots for (A) KI, (B) CsCl, and (C) acrylamide quenching of MscS mutants. The lines indicate the fit for the calculation of Stern−Volmer constant (K_{sv}) presented in Table 3. Data are shown for MscS WT (open square, solid line), W16 (closed circle, dash line), W251 (open upright triangle, dotted line), and W240 (closed inverted triangle, dash−dot line).

only W16 added to that containing both W240 and W251 results in a wild type spectrum because the latter residue allows an energy transfer (Figure 5B).

Quenching experiments performed on MscS mutants that contain only one Trp residue were performed with the quenchers KI, CsCl, and acrylamide and give an indication of the accessibility from the water phase (Figure 6 and Table 3). The results are in line with the positions of the fluorescence maxima described above. The quenchers have a small effect on W16 and W251 that have blue-shifted fluorescence maxima. This can be interpreted as a nonpolar surrounding shielded from the water phase. In contrast, W240 is more sensitive to the quenchers and the maximum is red-shifted as expected for a Trp exposed to the water phase. However, a small conformational change may be associated with the W251F mutation, since the purified MscS protein possessing only W240 (W16F/W251F) is more readily quenched by KI than is the wild type protein (Figure 6).

Significant amounts of dissociated MscS in the purification of the mutant W240L allowed us to compare spectroscopic properties of this form with the heptameric form (Figure 7). The fluorescence spectrum of the heptameric form is blue-

Table 3: Stern−Volmer Quenching Constants for MscS[a]

MscS mutant	Trp positions 16	240	251	K_{SV} (M^{-1}) acrylamide	KI	CsCl
WT	+	+	+	8.6	2.06	1.51
W240F/W251F	+	−	−	4.0	0.56	0.51
W16F/W240F	−	−	+	4.4	0.45	0.43
W16F/W251F	−	+	−	7.7	3.57	1.59
W251L	+	+	−	nd	2.49	1.7
W240L (heptamer)	+	−	+	nd	0.40	0.39
W240L (dissociated)	+	−	+	nd	1.45	1.2

[a] The Stern−Volmer quenching constant (K_{SV}) was determined from plots of the observed fluorescence measured in the presence and absence of the quenching agent. The protein fraction was the purified heptamer, except where indicated, when the dissociated material (**, Figure 4) was used; nd, not determined.

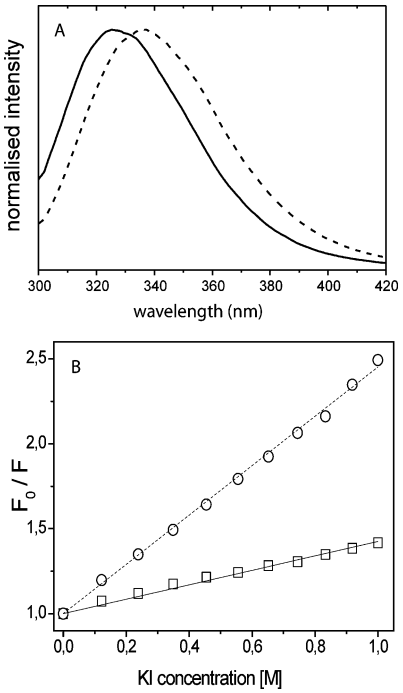

FIGURE 7: MscS monomers exhibit altered fluorescence. (A) Fluorescence spectra of the mutant MscS W240L in heptameric (solid line) and monomeric form (dash line). (B) Stern−Volmer plot for KI quenching of MscS W240L. The lines indicate the fit to the Stern−Volmer equation for the heptameric form (open square, solid line) and the dissociated form (open circle, dash line).

shifted as expected since this mutant contains only the shielded Trp residues W16 and W251 (see above). However, the peak of the dissociated form is red-shifted from 327 nm to 336 nm (Figure 7A), indicating a dramatic change in the environment: W251 in the heptamer is buried by residues from the adjacent subunit that are removed when MscS is dissociated. Quenching data support this analysis, since there is an increase in the Stern−Volmer quenching constant for the dissociated monomer (Table 3; Figure 7B).

DISCUSSION

Tryptophan residues frequently play critical roles in protein structure and function. The data presented here suggest critical roles for W16 and W240 in MscS-Ec, but a less significant role for W251. However, aromatic residues are required at all three positions, which is consistent with the known importance of these residues in protein structure. The most surprising result is the observation of the importance

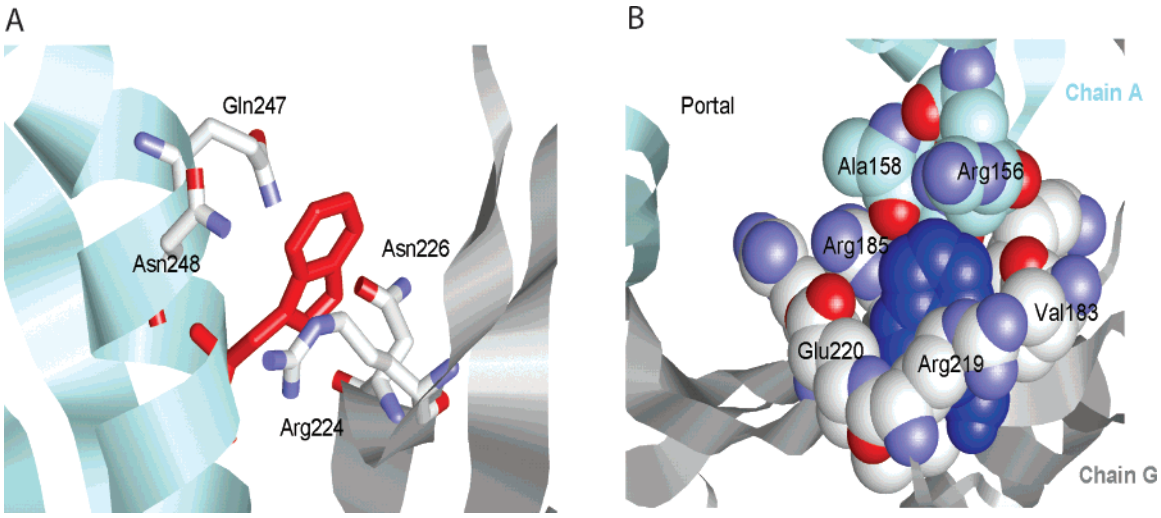

FIGURE 8: Neighboring residues of W240 and W251 in MscS. The residues that pack against the tryptophans are shown. (A) W251 (red) shown in the context of Asn, Gln, and Arg residues in stick representations using the ribbon presentation for the backbone of the protein. (B) W240 (blue) shown in a space-filling representation of the close-packed residues. The images were made with RasTop on the basis of the crystal structure (*15*).

of W16. Substitution of this residue with other amino acids, even with aromatic residues, modifies the gating behavior of the MscS-Ec channel. The lack of structural information for this region of the protein is a hindrance to understanding the basis of this change. Little conservation of length of the region immediately amino-terminal to TM1 exists, but an aromatic residue is frequently present (87/100 of the closest MscS-Ec homologues) and is most often absent when the sequence is extremely short (data not shown). W16 in MscS could have an anchoring function in the membrane because the first resolved amino acid in the crystal structure (Y27) is close to the water−lipid interface and is only 10 amino acids away from W16. Moreover, previous work has established that a Cys residue at position 9 (S9C) is spontaneously cross-linked in membranes (*31*), which may indicate that the Cys residues of adjacent subunits are close enough to the membrane surface to be substrates for the Dsb oxidoreductase system (*32*). The fluorescence experiments indicate an apolar, and shielded, environment for W16 in the detergent solubilized state. However, our experiments do not distinguish whether W16 is located inside the protein matrix, shielded by the protein surrounding, or at the hydrophobic protein surface, protected by the detergent micelle. It is intriguing that W16, which is far away from the hydrophobic seals in position 105 and 109, has such an influence on gating. However, W16 is highly conserved and it seems possible that this residue serves as a fixing point at the water−lipid interface, holding the movable, pressure-detecting TM helices TM1 and TM2. The introduction of Trp residues into the MscL channel protein at positions close to the head-groups increases the tension needed to gate the channel (*13*). The effects observed here are the opposite to that seen with MscL, since it is the removal of the Trp residue that increases the tension required to gate MscS-Ec. This points to a critical role of W16 in fixing the positions of the pressure-sensing TM1−TM2 helices so that they can respond to tension by making the structural transition that results in the open configuration.

W240 and W251 are far away from the water lipid interface but are important for the stability, and possibly assembly, of MscS-Ec. This conclusion is driven by the observed dependence of MscS on an aromatic residue (Trp, Phe, or Tyr) at positions 240 and 251: replacement with the hydrophobic Leu is not as effective since a W240L/W251L mutant does not integrate into the membrane. Although both of these Trp residues are found at the subunit interface, their environments are quite different. W251 is "caged" by Asn and Gln residues and is in close contact to R224 of the neighbor subunit (Figure 8A). Cation−π interactions (R224−W251) may stabilize the oligomeric state of MscS. We calculated the electrostatic part of the cation−π interaction between these residues to be an average value of $E_{es} = -5.1$ kcal/mol per subunit using the program CAPTURE (*33*) on the basis of the crystal structure (*15*). However, Phe is found more frequently at position 251 than Trp, R224 is not conserved, and the cage structure is only found in the very closest of homologues. Consequently, cation−π interactions involving W251 and the presence of the cage structure may be important for MscS-Ec, but are not general structural stability elements in the MscS family. However, we could not detect a change in oligomer stability for a mutation of R224 to Met (data not shown).

It is a remarkable observation that substitution of one amino acid, W240, has such a profound effect on MscS oligomer stability. The conservation of W240 and its position at the subunit interface is consistent with a role in stabilizing the oligomer (*5*, *34*). Our SDS−PAGE and the gel filtration results suggest that a substitution of W240 with Leu has a severe effect on stability and conformation. Bogan and Thorn showed that Trp residues are enriched in binding hot spots at protein interfaces more than any other amino acid (*5*). In the amended crystal structure, W240 is also located at the subunit interface (Figure 8B) (*15*). The R219 residue is ~5 Å away from W240 on the same subunit and is only moderately conserved (43/100 homologues with R/K at this position), however, these residues would not provide inter-subunit stabilization. Cation−π interactions may be important for MscS-Ec secondary structure, stabilizing the $\alpha\beta$ domain, but at present there are no obvious candidates for such inter-subunit interactions. The most significant stabilization at this position most probably arises from occlusion of bulk solvent (*5*), since the hydrophobic backbone of the highly conserved

R185 (98/100 sequences have Arg at this position) is packed against the ring structure of W240 from the same subunit (Figure 8B). In addition, this pair of residues interacts with Ala158 and Gly160 of the adjacent subunit and possibly Val183 of the same subunit. One side of the ring structure of W240 is exposed from the outside of the channel, but the opposite face is buried against the protein. Possibly the introduction of Leu at position 240 lowers MscS incorporation into the membrane because its smaller size reduces the stability of this hydrophobic patch. Two observations support this idea: the change in apparent mass in SDS−PAGE for W240L mutation toward the predicted value, which is consistent with the mutant protein being more readily unfolded by SDS, and the greater abundance of monomer in MscS purified in DDM.

The fine-tuning of the gating and increased stability of Trp-containing MscS are consistent with our understanding of the role of this rare amino acid in structure and activity of proteins. To develop Trp as a conformational probe for MscS and related proteins it is critical that replacement of the native Trp residues does not significantly perturb the structure and activity of the protein. A functional and stable MscS channel is formed when all Trp residues are exchanged against Phe, however, activity closer to the native channel is obtained when residue 16 is replaced with a Tyr. The W16Y/W240F/W251F channel exhibits wild type levels of protection of cells against hypoosmotic shock and gates at a tension threshold closer to the wild type. This provides the basis for further work to understand the gating of MscS-Ec and its interactions with the lipid environment (*35*−*37*).

REFERENCES

1. Burley, S. K., and Petsko, G. A. (1986) Amino-aromatic interactions in proteins, *FEBS Lett. 203*, 139−143.
2. Zacharias, N., and Dougherty, D. A. (2002) Cation-[pi] interactions in ligand recognition and catalysis, *Trends Pharmacol. Sci. 23*, 281−287.
3. Andersen, O. S., Greathouse, D. V., Providence, L. L., Becker, M. D., and Koeppe, R. E. (1998) Importance of Tryptophan Dipoles for Protein Function: 5-Fluorination of Tryptophans in Gramicidin A Channels, *J. Am. Chem. Soc. 120*, 5142−5146.
4. Killian, J. A., and von Heijne, G. (2000) How proteins adapt to a membrane-water interface, *Trends Biochem. Sci. 25*, 429−434.
5. Bogan, A. A., and Thorn, K. S. (1998) Anatomy of hot spots in protein interfaces, *J. Mol. Biol. 280*, 1−9.
6. Booth, I. R., Edwards, M. D., Black, S., Schumann, U., and Miller, S. (2007) Mechanosensitive channels in bacteria: signs of closure?, *Nat. Rev. Microbiol. 5*, 431−440.
7. Berrier, C., Coulombe, A., Szabo, I., Zoratti, M., and Ghazi, A. (1992) Gadolinium Ion Inhibits Loss of Metabolites Induced by Osmotic Shock and Large Stretch-Activated Channels in Bacteria, *Eur. J. Biochem. 206*, 559−565.
8. Levina, N., Totemeyer, S., Stokes, N. R., Louis, P., Jones, M. A., and Booth, I. R. (1999) Protection of Escherichia coli cells against extreme turgor by activation of MscS and MscL mechanosensitive channels: identification of genes required for MscS activity, *EMBO J. 18*, 1730−1737.
9. Schleyer, M., Schmid, R., and Bakker, E. P. (1993) Transient, specific and extremely rapid release of osmolytes from growing cells of Escherichia coli K-12 exposed to hypoosmotic shock, *Arch. Microbiol. 160*, 424−431.
10. Berrier, C., Besnard, M., Ajouz, B., Coulombe, A., and Ghazi, A. (1996) Multiple mechanosensitive ion channels from Escherichia coli, activated at different thresholds of applied pressure. *J. Membr. Biol. 151*, 175−187.
11. Li, Y., Moe, P. C., Chandrasekaran, S., Booth, I. R., and Blount, P. (2002) Ionic regulation of MscK, a mechanosensitive channel from Escherichia coli, *EMBO J. 21*, 5323−5330.
12. Sukharev, S. I., Sigurdson, W. J., Kung, C., and Sachs, F. (1999) Energetic and spatial parameters for gating of the bacterial large conductance mechanosensitive channel, MscL, *J. Gen. Physiol. 113*, 525−540.
13. Chiang, C. S., Shirinian, L., and Sukharev, S. (2005) Capping transmembrane helices of MscL with aromatic residues changes channel response to membrane stretch, *Biochemistry 44*, 12589−12597.
14. Bass, R. B., Strop, P., Barclay, M., and Rees, D. C. (2002) Crystal structure of Escherichia coli MscS, a voltage-modulated and mechanosensitive channel, *Science 298*, 1582−1587.
15. Steinbacher, S., Bass, R., Strop, P., and Rees, D. C. (2007) Structures of the Prokaryotic Mechanosensitive Channels MscL and MscS, *Curr. Topics Membr. 58*, 1−24.
16. Miller, S., Bartlett, W., Chandrasekaran, S., Simpson, S., Edwards, M., and Booth, I. R. (2003) Domain organization of the MscS mechanosensitive channel of Escherichia coli, *EMBO J. 22*, 36−46.
17. Booth, I. R., Edwards, M. D., Black, S., Schumann, U., Bartlett, W., Rasmussen, T., Rasmussen, A., and Miller, S. (2007) Physiological Analysis of Bacterial Mechanosensitive Channels, in *Methods in Enzymology* (Sies, M., and Haeussinger, D., Eds.) pp 47−61, Elsevier, New York.
18. Schumann, U., Edwards, M. D., Li, C., and Booth, I. R. (2004) The conserved carboxy-terminus of the MscS mechanosensitive channel is not essential but increases stability and activity, *FEBS Lett. 572*, 233−237.
19. Edwards, M. D., Li, Y., Kim, S., Miller, S., Bartlett, W., Black, S., Dennison, S., Iscla, I., Blount, P., Bowie, J. U., and Booth, I. R. (2005) Pivotal role of the glycine-rich TM3 helix in gating the MscS mechanosensitive channel, *Nat. Struct. Mol. Biol. 12*, 113−119.
20. Vasquez, V., Cortes, D. M., Furukawa, H., and Perozo, E. (2007) An Optimized Purification and Reconstitution Method for the MscS Channel: Strategies for Spectroscopical Analysis, *Biochemistry 46*, 6766−6773.
21. Gill, S. C., and von Hippel, P. H. (1989) Calculation of protein extinction coefficients from amino acid sequence data, *Anal. Biochem. 182*, 319−326.
22. Kirby, E. P., and Steiner, R. F. (1970) The tryptophan microenvironments in apomyoglobin, *J. Biol. Chem. 245*, 6300−6306.
23. Altschul, S. F., Madden, T. L., Schaffer, A. A., Zhang, J. H., Zhang, Z., Miller, W., and Lipman, D. J. (1997) Gapped BLAST and PSI-BLAST: a new generation of protein database search programs, *Nucleic Acids Res. 25*, 3389−3402.
24. Blount, P., Sukharev, S. I., Schroeder, M. J., Nagle, S. K., and Kung, C. (1996) Single residue substitutions that change the gating properties of a mechanosensitive channel in Escherichia coli, *Proc. Natl. Acad. Sci.U.S.A. 93*, 11652−11657.
25. Blount, P., Schroeder, M. J., and Kung, C. (1997) Mutations in a bacterial mechanosensitive channel change the cellular response to osmotic stress, *J. Biol. Chem. 272*, 32150−32157.
26. Ou, X., Blount, P., Hoffman, R. J., and Kung, C. (1998) One face of a transmembrane helix is crucial in mechanosensitive channel gating, *Proc. Natl. Acad. Sci. U.S.A. 95*, 11471−11475.
27. Heuberger, E. H., Veenhoff, L. M., Duurkens, R. H., Friesen, R. H., and Poolman, B. (2002) Oligomeric state of membrane transport proteins analyzed with blue native electrophoresis and analytical ultracentrifugation, *J. Mol. Biol. 317*, 591−600.
28. Callis, P. R., and Liu, T. (2004) Quantitative prediction of fluorescence quantum yields for tryptophan in proteins, *J. Phys. Chem. B 108*, 4248−4259.
29. Eftink, M. R. (1991) Fluorescence techniques for studying protein structure, *Methods Biochem. Anal. 35*, 127−205.
30. Stryer, L., and Haugland, R. P. (1967) Energy Transfer: A Spectroscopic Ruler, *PNAS 58*, 719−726.
31. Miller, S., Edwards, M. D., Ozdemir, C., and Booth, I. R. (2003) The closed structure of the MscS mechanosensitive channel− Cross-linking of single cysteine mutants, *J. Biol. Chem. 278*, 32246−32250.
32. Kadokura, H., Katzen, F., and Beckwith, J. (2003) Protein disulfide bond formation in prokaryotes, *Annu. Rev. Biochem. 72*, 111−135.
33. Gallivan, J. P., and Dougherty, D. A. (1999) Cation-pi interactions in structural biology, *PNAS 96*, 9459−9464.
34. Clackson, T., and Wells, J. A. (1995) A hot spot of binding energy in a hormone-receptor interface, *Science 267*, 383−386.

35. Powl, A. M., Carney, J., Marius, P., East, J. M., and Lee, A. G. (2005) Lipid interactions with bacterial channels: fluorescence studies, *Biochem. Soc. Trans. 33*, 905−909.
36. Powl, A. M., East, J. M., and Lee, A. G. (2003) Lipid-protein interactions studied by introduction of a tryptophan residue: The mechanosensitive channel MscL, *Biochemistry 42*, 14306−14317.
37. Powl, A. M., East, J. M., and Lee, A. G. (2005) Heterogeneity in the binding of lipid molecules to the surface of a membrane protein: hot spots for anionic lipids on the mechanosensitive channel of large conductance MscL and effects on conformation, *Biochemistry 44*, 5873−5883.

BI701056K